# Modeling and Animating Eye Blinks

LAURA C. TRUTOIU and ELIZABETH J. CARTER, Carnegie Mellon University
IAIN MATTHEWS, Disney Research, Pittsburgh and Carnegie Mellon University
JESSICA K. HODGINS, Carnegie Mellon University and Disney Research, Pittsburgh

Facial animation often falls short in conveying the nuances present in the facial dynamics of humans. In this article, we investigate the subtleties of the spatial and temporal aspects of eye blinks. Conventional methods for eye blink animation generally employ temporally and spatially symmetric sequences; however, naturally occurring blinks in humans show a pronounced asymmetry on both dimensions. We present an analysis of naturally occurring blinks that was performed by tracking data from high-speed video using active appearance models. Based on this analysis, we generate a set of key-frame parameters that closely match naturally occurring blinks. We compare the perceived naturalness of blinks that are animated based on real data to those created using textbook animation curves. The eye blinks are animated on two characters, a photorealistic model and a cartoon model, to determine the influence of character style. We find that the animated blinks generated from the human data model with fully closing eyelids are consistently perceived as more natural than those created using the various types of blink dynamics proposed in animation textbooks.

Categories and Subject Descriptors: I.3.7 [**Computer Graphics**] Three-Dimensional Graphics and Realism

General Terms: Measurement, Human Factors

Additional Key Words and Phrases: Eye blinks

**ACM Reference Format:**

Trutoiu, L. C., Carter, E. J., Matthews, I., and Hodgins, J. K. 2011. Modeling and animating eye blinks. ACM Trans. Appl. Percept. 8, 3, Article 17 (August 2011), 17 pages.
DOI = 10.1145/2010325.2010327 http://doi.acm.org/10.1145/2010325.2010327

## 1. INTRODUCTION

Facial animation requires laborious attention to detail because humans are attuned to subtle changes and anomalies in faces. In particular, eye motion, gaze, saccades, and blinks generally require significant artist input. Failure to properly animate eye motion may alter the intended emotional content of animated feature films. *Beowulf* is an example of an animated movie that reviewers describe as lacking "the spark of true life" in the moving faces [Dargis 2007]. In this article, we focus on generating and evaluating parameters for eye blinks (Figure 1), one important component of facial animation.

Partial support was provided by NSF CCF-0811450.
Authors' addresses: L. C. Trutoiu (corresponding author) E. J. Carter and J. K. Hodgins, Robotics Institute, Carnegie Mellon University, 5000 Forbes Ave., Pittsburgh, PA 15213; email: ltrutoiu@cs.cmu.edu; I. Matthews, Disney Research 4720 Forbes Ave., Lower Level, Suite 110, Pittsburgh, PA 15213.

DOI 10.1145/2010325.2010327 http://doi.acm.org/10.1145/2010325.2010327

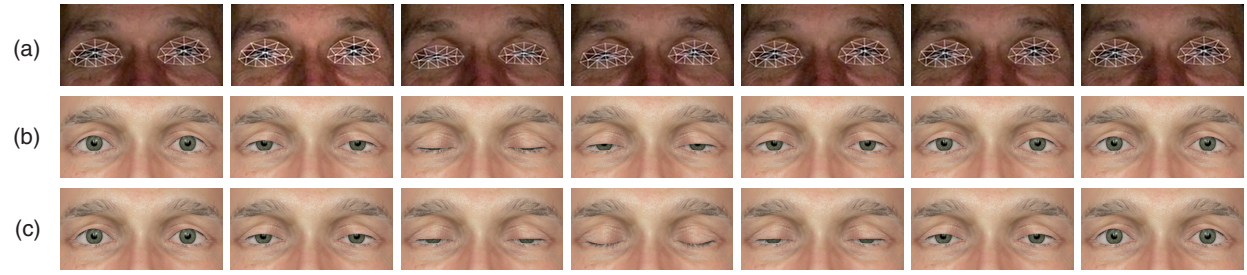


Fig. 1. (a) High-speed video footage of human blinks was tracked with Active Appearance Models. (b) Based on the tracked data, a realistic model of human eye blinks was used to generate eye blink animations. (c) The symmetric blinks generated using common animation guidelines.

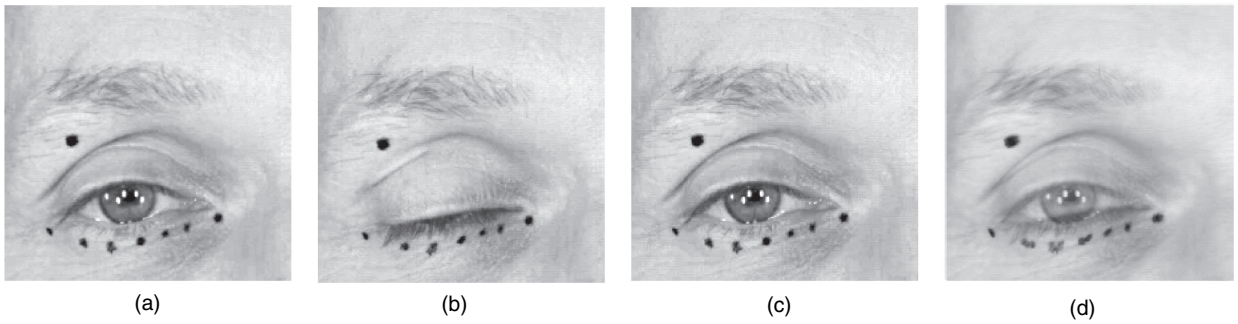


Fig. 2. Images of the eye at: (a) the beginning of the eye blink, (b) the maximum closed position, and (c) the end of the blink. (d) Overlaid images of the eye during blinking. The blurring of the markers on the lower eyelid demonstrates the displacement of the lower eyelid during the eye blink.

Highly skilled animators can convey a wide range of emotions using subtle animation cues, including eye blink amplitudes and dynamics. Indeed, animation textbooks recommend using blinks as a way to "add life to a character" and to emphasize or influence personality and mood [Maestri 1996]. Unfortunately, the quality of an animation can suffer when incorrect assumptions are made about the dynamics of eye blinks. These simplifications include the directive that blinks are symmetric; therefore, the same number of frames should be used for opening and closing the eyelids [Culhane 1988; Maestri 1996]. Additionally, it has been suggested that a linear or near-linear velocity profile for the eyelid motion is sufficient [Culhane 1988; Maestri 1996; Williams 2001]. In practice, 3D animation systems often make use of ease-in/ease-out animation profiles for motions, including eye blinks. However, simple ease-in/ease-out motions do not accurately mimic human eyelid motion. Furthermore, 300 frames per second (fps) video makes it clear that there is nonnegligible horizontal and vertical movement of the lower eyelid, as shown in Figure 2. This horizontal motion is not mentioned in the textbooks.

We challenge the common assumptions about animating eye blinks and show results indicating that observers distinguish and rate as more natural eye blink animations that are generated from actual human data. We propose using data-driven methods for inferring parameters in traditional facial animation techniques, such as blend shape animation. We use the Active Appearance Model (AAM) computer vision algorithm [Matthews and Baker 2004] to track unadorned eyes in high-speed video footage (Figure 1). The tracking information allows us to determine the accurate temporal and spatial dimensions of human blinks. We use a model based on Principal Component Analysis (PCA) that can generate new blinks in the same space as the training data. An extensive set of perceptual

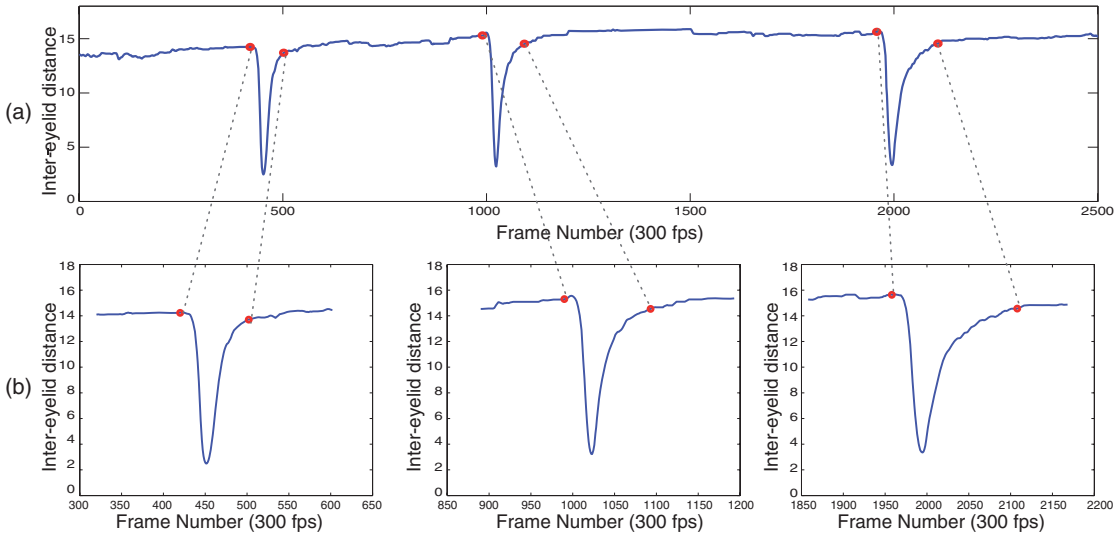


Fig. 3. (a) A sequence (8.3 seconds) of inter-eyelid distance data. (b) Individual human eye blinks are characterized by a fast eyelid closing and a slower, asymptotically converging eyelid opening.

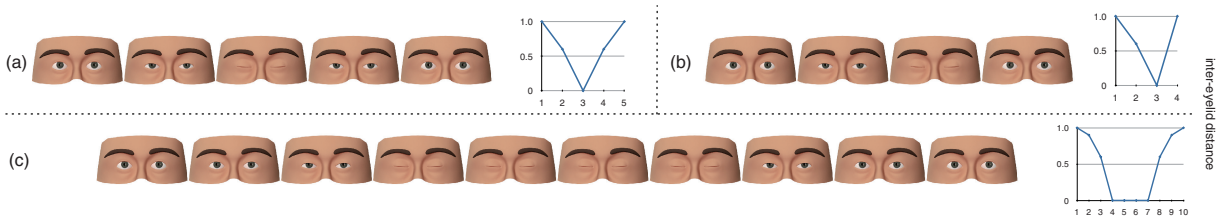


Fig. 4. Illustrative figure of the animation timing suggested for a blink adapted from Maestri [1996]. (a) Temporally and spatially symmetric sequence that the author recommends for most situations. (b) A second, asymmetric, blink is used by the author to illustrate how to make the character look more alert. Note that the resulting dynamics are a reversal of human eye blink dynamics (as shown in Figure 2). (c) A long blink sequence that is fully symmetric and creates the appearance of sleepiness. None of these blinks accurately models spontaneous human eye blink motion.

experiments shows the improvements in naturalness ratings that arise from the use of accurate eye blink motion. A set of representative eye blink profiles from video data are shown in Figure 3 while Figure 4 shows examples of eye blink profiles used in animation.

## 2. RELATED WORK

Facial movements and expressions are of interest to animators, computer graphics researchers, psychologists, and neuroscientists. In this section, we review three topics pertaining to eye motions and blinking: the physiology of human eye blinks, methods for measuring eyelid dynamics, and common animation methods.

### 2.1 Physiology of Eye Blinks

Blinking is a natural eye motion defined as the rapid closing and opening of the eyelid [Blount 1928]. Two antagonistic muscles are primarily responsible for generating a blink: the sphincter muscle, orbicularis oculi, closes the eyelids, and the levator palpebrae superiori muscle raises the upper lid

[Evinger et al. 1991]. Eye blinks can be put into three categories: spontaneous (unconsciously triggered), reflexive (elicited by a sudden impulse), and voluntary (intentionally triggered). These categories can be distinguished based on duration, amplitude, and context [Bacher and Smotherman 2004]. Throughout this study, we focus on naturally occurring, spontaneous blinks.

The dynamics of lid motion follow a highly asymmetrical motion pattern in time (Figure 3). The down phase, when the lid closes, is short in duration and achieves a high velocity with fast accelerations. The up phase lasts longer and decelerates more slowly. This pattern has been described by multiple research groups [Evinger et al. 1984; Guitton et al. 1991; Sun et al. 1997; VanderWerf et al. 2003]. The duration and variability of blinks have been recorded under various conditions, including voluntary and spontaneous blinks as well as those induced by air puffs and electrical stimuli. Typical dynamics for a spontaneous blink are shown in Figure 3. Note that accurately determining the end point of a blink is difficult because the eye opens slowly and the final inter-eyelid distance does not always return to the initial inter-eyelid distance in a brief amount of time. VanderWerf and colleagues [2003] proposed defining the end of a blink as the instant when the inter-eyelid distance reaches 95% of the original value.

Changes in the speed, frequency, and strength of blinks provide information to the observer. For example, increased durations of eye closure and reopening are associated with drowsiness [Caffier et al. 2003]. Blink rate is positively correlated with difficulty for some tasks, such as mental arithmetic [Tanaka and Yamaoka 1993], and negatively correlated for others, including flight simulation tasks [Veltman and Gaillard 1998; Wilson et al. 1987]. Additionally, both blink frequency and blink duration have been associated with emotional states. For example, the amplitude of reflexive blinks was higher while viewing unpleasant pictures than during pleasant pictures [Codispot et al. 2001]. Cues from blinking can also suggest whether or not a subject is telling the truth. Elevated blink rates are found in individuals who are masking their true emotions [Porter and ten Brinke 2008], and people show decreased blinking while lying, followed by increased blinking afterwards [Leal and Vrij 2008].

### 2.2 Quantifying Eye Blink Dynamics

Evinger and colleagues [1984] described two methods for measuring eyelid position: scleral search coils and electromyographic (EMG) recordings. The scleral search coils required insertion under anesthesia and a head restraint; therefore, they were used only in animals. For humans, EMG recordings were performed using electrodes pasted to the upper eyelid. More recently, researchers have performed human eyelid recordings using the electromagnetic search coil technique, which involves positioning the participant in the center of a weak magnetic field, taping one or two coils to the eyelid, and recording changes in the current [Evinger et al. 1991; Sun et al. 1997; VanderWerf et al. 2003]. This method produces measures of blink amplitude, velocity, duration, rate, and time of occurrence. Moreover, it can measure the horizontal and vertical movements of both the upper and lower eyelid [VanderWerf et al. 2003]. However, it is limited by the number of coils that can be used simultaneously, and participants might change their behavior because of the invasiveness of the procedure. Additionally, recordings must be done while the participant remains still inside the magnetic field. These limitations make it impractical for use in many settings, including those used for performance capture. Video is a rich source of information for measuring eye blink dynamics. For example, Bacivarov and colleagues [2008] have shown that active appearance models can be successfully used to detect eye blink events in video, and our approach is similar.

### 2.3 Eye Blink Animation

Few data-driven methods for eye blink animation exist. One of the seminal works on eye motion animation proposed a model for eye movements that used empirical models of saccades and statistical

models of eye-tracking data, including when blinks are triggered [Lee et al. 2002]. However, their model provided no information regarding the dynamics of the eye blink.

Deng and colleagues [2005] proposed a texture synthesis-based technique to simultaneously generate realistic eye gaze and blink motion by modeling the correlation between eye gaze and blink motion. A video of one actor wearing face markers was tracked. Independent blink profiles generated with this motion appear similar to our data. However, their approach did not assess the benefits of accurate eye blink profiles. Steptoe and colleagues [2010] investigated the kinematics of blinks and eyelid saccades. They used frames from video recordings (taken at 60 fps) of one individual during three blinks and three eyelid saccades to produce similar-looking animations with fully closed eyelids for the blinks and slightly closed eyelids for the saccades. These blink and saccade animations were then compared in a perceptual study to animations generated using the equations derived by Evinger and colleagues [1991] and animations created using linear interpolation. Ten participants from their research group ranked the realism of exemplars of each type of animation using their memory of real blink dynamics and then ranked them based on their similarity to an eye movement from the source video. The animations generated from the video were ranked highest for realism and similarity to the source, followed by the clips created from the equations and then the sequences generated using linear interpolation. Unfortunately, they did not assess the blinks and saccades separately. Only six stimuli (three blinks and three saccades) from each category were assessed, and they did not examine the full range of variability in blink duration and eyelid closing amplitudes seen in human eye blinks.

## 3. APPROACH

Unlike previous methods, the experimental framework we propose relies on high-resolution temporal and spatial measures of eye blink dynamics and we use perceptual experiments to validate the measured and modeled dynamic behaviors. Because we are quantifying both temporal and spatial characteristics, the results of this framework can easily replace or complement existing blink animation techniques. For example, traditional animation curves can be used to reproduce the eye blink dynamics that we have derived from data.

### 3.1 Active Appearance Model Video Analysis

Active Appearance Models are a nonrigid deformable tracking method that has been successfully used to track dynamic facial expressions [Cootes et al. 1998; Matthews and Baker 2004]. The model consists of two parts, a linear model of shape deformation and a linear model of shape-normalized appearance change, which are typically learned using PCA from labeled training data. Our AAM model tracks only the eyes of a given actor and is learned from a handful (20–25) of manually labeled images of each actor. Following the notation of Matthews and Baker [2004], the shape, $\boldsymbol{s}$, of the AAM is the vector of vertices used to describe both eyes,

$$\boldsymbol{s} = (x_1, y_1, x_2, y_2, \ldots, x_v, y_v)^{\mathrm{T}}. \tag{1}$$

We label $v = 18$ 2D points in each training image as shown in Figure 5. The linear shape model is defined as

$$\boldsymbol{s} = \boldsymbol{s}_0 + \sum_{i=1}^{n} p_i \boldsymbol{s}_i, \tag{2}$$

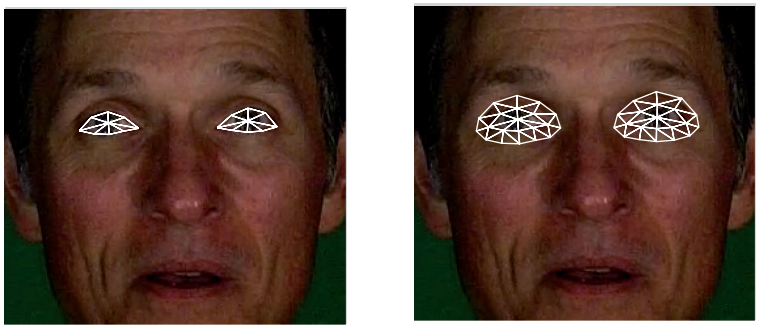

(a) (b)

Fig. 5. (a) Basic eighteen point template used for video AAM labeling and tracking. (b) The basic template can be augmented to 42 points by adding border vertices.

where $\boldsymbol{s}_0$ is the mean shape, $\boldsymbol{s}_i$ are the shape PCA basis vectors, and $p_i$ are the shape parameters. The appearance model is similarly defined as

$$A(\boldsymbol{x}) = A_0(\boldsymbol{x}) + \sum_{i=1}^{m} \lambda_i A_i(\boldsymbol{x}) \qquad \forall \boldsymbol{x} \in \boldsymbol{s}_0, \tag{3}$$

where $A_0(\boldsymbol{x})$ is the mean appearance, $A_i(\boldsymbol{x})$ are the PCA appearance basis vectors, and $\lambda_i$ are the appearance parameters. We let $\boldsymbol{s}_0$ also denote the set of pixels $\boldsymbol{x} = (x, y)^{\mathrm{T}}$ that lie inside the base mesh $\boldsymbol{s}_0$. The appearance of an AAM is then an image $A(\boldsymbol{x})$ defined over the pixels $\boldsymbol{x} \in \boldsymbol{s}_0$. The original formulation of AAMs [Cootes et al. 1998] included an additional PCA step to learn a single *coupled* parameterization of shape and appearance:

$$\boldsymbol{s} = \boldsymbol{s}_0 + \sum_{i=1}^{l} c_i w_p^{-1} \boldsymbol{s}_i \boldsymbol{j}_i^{\boldsymbol{s}}, \; A(\boldsymbol{x}) = A_0(\boldsymbol{x}) + \sum_{i=1}^{l} c_i A_i(\boldsymbol{x}) \boldsymbol{j}_i^{A(\boldsymbol{x})}. \tag{4}$$

The coupled parameters, $\boldsymbol{c} = (c_1, c_2, \ldots, c_l)^T$ are the parameter weights for the PCA basis of the concatenation of $\boldsymbol{p}$ and $\boldsymbol{\lambda}$:

$$\boldsymbol{c} = \begin{bmatrix} w_p \boldsymbol{p} \\ \boldsymbol{\lambda} \end{bmatrix} = USV^T = \boldsymbol{j} S V^T, \tag{5}$$

where $\boldsymbol{p} = (p_1, p_2, \ldots, p_n)^T$, $\boldsymbol{\lambda} = (\lambda_1, \lambda_2, \ldots, \lambda_m)^T$, $w_p$ is an energy normalizing weight, and $\boldsymbol{j} = (\boldsymbol{j}_1, \boldsymbol{j}_2, \ldots, \boldsymbol{j}_l)$ are the eigenvectors of the joint PCA basis. For applications where shape and appearance are highly correlated, such as eyelid tracking, the coupled parameterization can be significantly more compact, that is, $l < m + n$.

For tracking faces, Matthews and Baker [2004] do not use the coupled parameterization. The independent parameterization allowed them to introduce the fast, appearance *project out*, inverse-compositional, gradient descent fitting algorithm. However, for eyelid tracking, the coupled model has many advantages. For example, our model has $n = 8$ shape parameters (98% variance), $m = 10$ appearance parameters (90%), but only $l = 10$ coupled parameters (98%). Fewer parameters make the tracking faster and more reliable.

To accurately and efficiently fit a coupled-parameter AAM model to an image, we extend the *simultaneous* shape and appearance, inverse-compositional, gradient descent fitting algorithm described by

Baker and colleagues [2003],

$$\sum_{\mathbf{x}} \left[ A_0(\mathbf{W}(\mathbf{x};\Delta\mathbf{p})) + \sum_{i=1}^{m} (\lambda_i + \Delta\lambda_i) A_i(\mathbf{W}(\mathbf{x};\Delta\mathbf{p})) - I(\mathbf{W}(\mathbf{x};\mathbf{p})) \right]^2$$

where $\mathbf{W}(\mathbf{x};\mathbf{p})$ denotes the piecewise affine warp over each triangle of the AAM mesh deformed by the shape parameters $\boldsymbol{p}$. We replace the independent shape and appearance parameterization with the coupled parameters and solve for the incremental warp update

$$\Delta\mathbf{c} = -H^{-1} \sum_{\mathbf{x}} \mathbf{SD}^{\mathrm{T}}(\mathbf{x}) E(\mathbf{x}), \tag{6}$$

where the coupled-parameters *steepest descent images* are given by

$$\mathbf{SD}(\mathbf{x}) = \left[ \left( \nabla A_0 + \sum_{i=1}^{l} c_i \nabla A_i \mathbf{j}_i^{\boldsymbol{\lambda}} \right) \frac{\partial \mathbf{W}}{\partial c_1}, \ldots, \left( \nabla A_0 + \sum_{i=1}^{l} c_i \nabla A_i \mathbf{j}_i^{\boldsymbol{\lambda}} \right) \frac{\partial \mathbf{W}}{\partial c_n} \right] + \left[ A_1(\mathbf{x}) \mathbf{j}_i^{A(\mathbf{x})}, \ldots, A_m(\mathbf{x}) \mathbf{j}_i^{\boldsymbol{\lambda}} \right],$$

where $\mathbf{j}_i^{\boldsymbol{\lambda}}$ denotes the subset of $\mathbf{j}_i$ that is modified by $\boldsymbol{\lambda}$ in (5),

$$H^{-1} = \sum_{\mathbf{x}} \mathbf{SD}^{\mathrm{T}}(\mathbf{x}) \mathbf{SD}(\mathbf{x}) \tag{7}$$

is the Gauss-Newton approximation to the Hessian, and the coupled parameter AAM error function is

$$E(\mathbf{x}) = A_0(\boldsymbol{x}) + \sum_{i=1}^{l} c_i A_i(\boldsymbol{x}) \boldsymbol{j}_i^{\boldsymbol{\lambda}} - I(\mathbf{W}(\mathbf{x};\mathbf{c})). \tag{8}$$

### 3.2 Data Processing

Three actors were recruited from the local community to record the video stimuli for this study (Figure 6). We recorded videos at 300 fps with a Casio Exilim FX1 camera. The actors were instructed to perform several two-minute vignettes, and video data was recorded during both the performances and the breaks in between.

Each video sequence at 300 fps was over 400,000 frames in length. For each actor's sequence, a small number of frames were manually labeled with 18 points as shown in Figure 5(a). The data was then tracked using the method described before. We automatically extend the eye model to include the additional border vertices shown in Figure 5(b), resulting in a 42-point shape model. Because the data is 300 fps and does not change much between frames, tracking is very reliable and fast. Our implementation runs at over 200 fps and is able to track an entire 400,000 frame sequence given an initial estimate for the first frame.

Blink frequency and interblink timing were quantified for the three actors shown in Figure 6. Blink frequency varied across the three actors: Actor 1 had an average blink rate of 8.2 blinks per minute, Actor 2 had an average blink rate of 27.0 blinks per minute, and Actor 3 had an average rate of 6.6 blinks per minute. Though all of the blink rates are within previously reported bounds [Doughty 2001], Actor 2 showed a relatively increased blink frequency, possibly due to wearing contact lenses. Further analysis can be conducted on the timing of eye blinks; however, the scope of this article is to investigate the dynamics of independent eye blinks.

### 3.3 Animated Blink Profiles

A basic model of an eye blink profile can be characterized as the inter-eyelid distance over time. For our perceptual experiments, we generate animations using six profile types. Two of the profiles (real

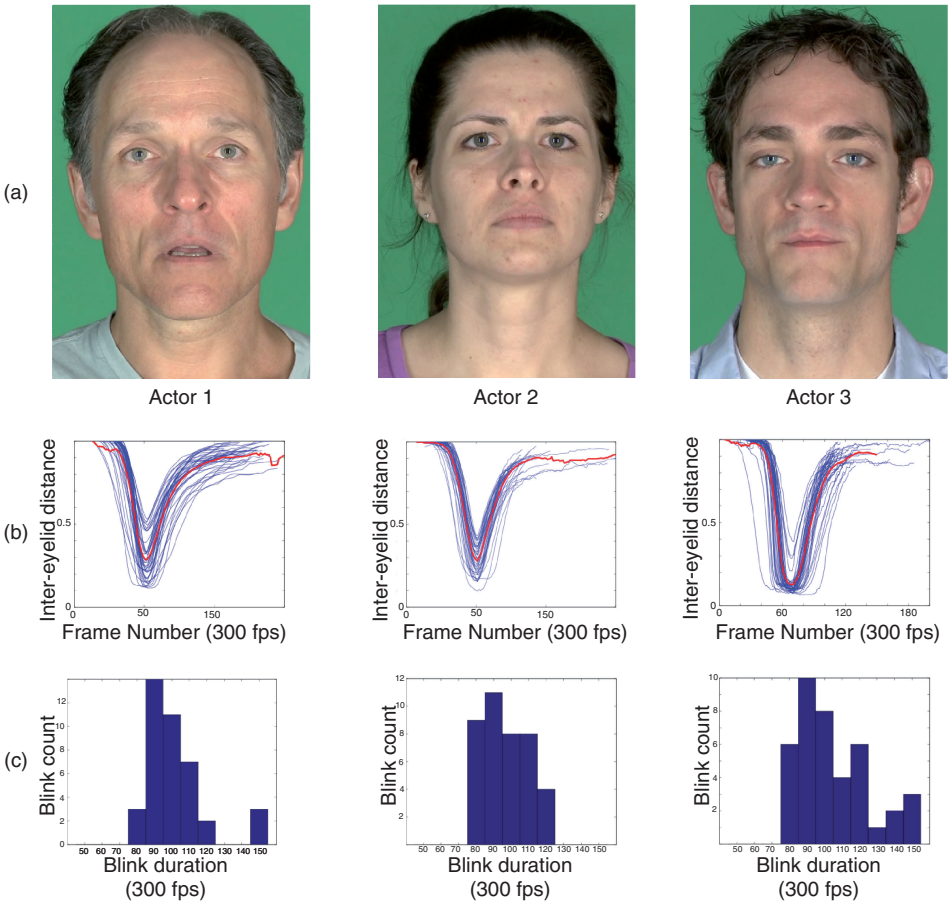


Fig. 6. (a) Video data from three actors was used in this study. (b) For each actor, 40 eye blinks were aligned according to the minimum inter-eyelid distance to depict the variability in closing amplitude. The mean blink for each actor (red) was calculated by averaging the 40 blinks after alignment. (c) Histograms of blink durations.

and model) were created using tracked video data; the other four are based on traditional animation techniques (symmetric linear, asymmetric linear, ease-in/ease-out symmetric, and ease-in/ease-out asymmetric).

3.3.1 *Real Profiles.* The inter-eyelid distance of Actor 1 was calculated from the AAM tracked video data (300 fps) as the absolute distance between a horizontally centered upper eyelid marker and a horizontally centered lower eyelid marker. For the purpose of this study, we assumed that the motion of both eyes was identical. A zero-phase 10-frame filter was first applied to the signal. An automatic blink-labeling algorithm was used to identify the local minima in the inter-eyelid distance signal. The local minima correspond to periods when the eyes are closed, with a distance close to zero between the upper and lower eyelid. The algorithm then looked in the neighborhood of each minimum point (300 frames to the left and 300 frames to the right of the minima) for the beginning and end of the eye blink based on two criteria.

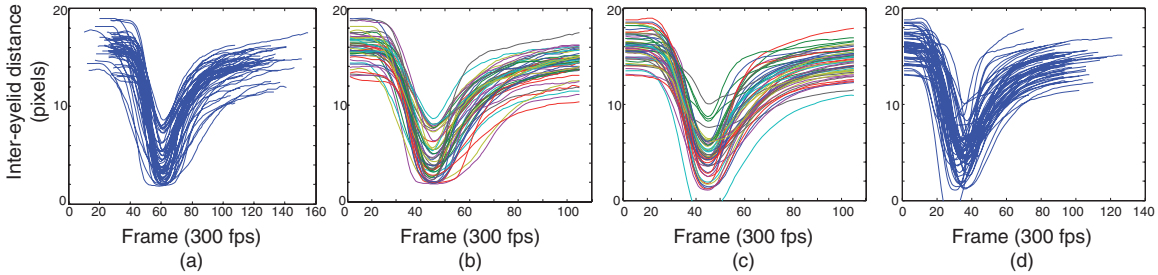


Fig. 7. PCA-based eye blink model. (a) The blink model takes as input blink profiles derived from video. (b) The blinks are then normalized to the average blink length independently for opening and closing. (c) The PCA-based model then generates length-normalized blinks and scaling factors that are used to (d) generate blink profiles with the appropriate duration.

(1) The gradient of the inter-eyelid distance is small. The gradient is measured as the change in consecutive values of the inter-eyelid distance and is averaged over a window of 10 frames. Small values ($<0.1$) of the averaged gradient ensure that, over the given window, the inter-eyelid distance is constant, corresponding to little to no vertical motion in the eyelids.

(2) The inter-eyelid distance value is above the baseline value computed for each blink. The baseline value is defined as the average of the inter-eyelid distance over 100 frames left and right of the minima. Though eye blinks are shorter than 200 frames, the baseline value quantifies the average inter-eyelid distance over a window that contains the opening or closing of the eye. In this way, we ensure that the frames in the immediate vicinity of the eye-closed frame, which may have a small gradient but also have a value smaller than the baseline, are not labeled as the start or end of the blink.

To find the beginning of an eye blink we start at a local minimum and search backward. The first point located before the minimum that matches the two criteria listed corresponds to the instant the eyes begin to close. Similarly, starting at the minimum and searching forward, we can find the end of the eye blink (corresponding to the eye open position). Examples of the resulting start and end eye blink labels can be seen in Figure 3.

We supplemented the automatic blink annotation with visual inspection to remove false positives from the data (three segments) and verify the accuracy of the blink-labeling algorithm. Furthermore, observations of the video and audio content led us to recognize that some blinks were used as nonverbal communication. For several eye-closing points, the action was intended to represent a particular emotion, such as pride. These eye-closing intervals were removed from the dataset to ensure that only spontaneous blinks were used. The eye blink time series that were used in the subsequent experiments consist of 49 blinks from one male actor, collected over a six-minute period. To determine whether the blinks from this subject were idiosyncratic, we analyzed the blinks from two young adults, one male and one female. The blink profiles for all three actors are similar in both general shape, blink duration distribution, and closing amplitude. Figure 6 shows the histograms of blink duration and variability in closing amplitudes for the three actors.

3.3.2 *Model Profiles.* The blink sequences from Actor 1 were used to build a model that can generate different blink durations. For each blink, two splines, one each for eye closing and eye opening, are fit to the inter-eyelid position data at 300 fps. This technique allows the signals to be normalized for length and aligned such that the minimum inter-eyelid distance always occurs at the same frame (Figure 7). The normalized and aligned data matrix is augmented with the scaling factors that were used for the two blink parts. A PCA model then uses the first five dimensions (representing 98%

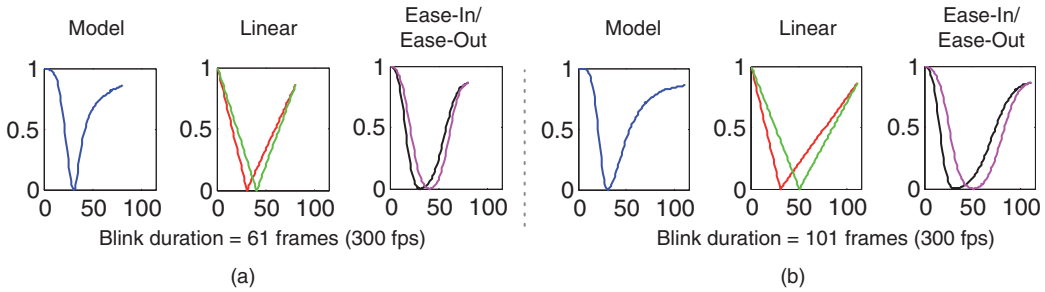


Fig. 8. Eye blink profiles: model (blue), symmetric linear (green), asymmetric linear (red), symmetric ease-in/ease-out (purple), and asymmetric ease-in/ease-out (black). Two different blink durations (a) 61 frames and (b) 101 frames are shown at 300 fps.

variance) to generate new signals by projecting new, random coefficients that are within one standard deviation of the coefficients to the PCA space. Animated blinks generated using this profile were used in all three experiments.

3.3.3 *Linear Profiles.* The linear blink profiles are generated by linearly interpolating between the inter-eyelid position at the beginning of the blink to the maximally closed position and from there to the end of the eye blink (Figure 8(a)). Two types of linear profiles can be generated: symmetric and asymmetric. The minimum inter-eyelid distance falls in the center frame for the symmetric linear profiles and in an off-center frame for the asymmetric linear profiles. These simple profiles of blink dynamics have been described in textbooks [Maestri 1996].

3.3.4 *Ease-In/Ease-Out Profiles.* Ease-in/ease-out (Figure 8) curves are often used in animation as a way of portraying motion accelerations and decelerations. Motion with ease-in/ease-out is thought to convey a greater sense of realism because it obeys physical laws for inertia. The generated ease-in/ease-out profiles are Bezier curves with control points proportional to the length of the two parts of the blink.

## 4. PERCEPTUAL STUDIES

Three perceptual studies were conducted to investigate the perceived naturalness of animated blinks. The animated clips were displayed on a 23-inch LCD display at actual size, where the inter-ocular distance equals 6 cm and the maximum inter-eyelid distance equals approximately 1.1 cm. For all experiments, only the eye region was visible (see Figure 1). Trials were self-initiated: the participants pressed a key to play each clip. Before every experiment, there was a brief practice session to familiarize the participants with the procedures. The experimental procedure was approved by the Institutional Review Board, and participants were compensated for their time.

### 4.1 Experiment 1: Comparing Eye Blinks Created with Tracked Data to our Profile Generation Method

Experiment 1 confirmed the validity of the PCA-based model by comparing the perceived naturalness of model-generated eye blinks to the perceived naturalness of those that were animated based on the data obtained from the video sequences. In this experiment, we also investigated the effects of motion blur in rendering and the effect of closing amplitude. Eye blink naturalness ratings were collected for two 3D animated characters, one photorealistic, one cartoon-like.

We hypothesized that the animated blinks with motion blur would be rated as more natural than animated blinks without motion blur. Furthermore, we expected that the difference in naturalness

Table I. Experiment 1 Results

| | Condition | Mean(SE) | F | p |
|---|---|---|---|---|
| Character | Cartoon | 4.04 (0.12) | 5.917 | 0.02 |
| | Photorealistic | 4.36 (0.16) | | |
| Profile | Model | 4.31 (0.12) | 39.07 | <0.001 |
| | Real | 4.10 (0.13) | | |
| Blur | MB | 4.18 (0.13) | 0.95 | 0.34 |
| | NB | 4.22 (0.13) | | |
| Amplitude | NC | 3.93 (0.15) | 15.55 | <0.001 |
| | FC | 4.46 (0.14) | | |

ratings between fully closed and naturally closed eye blinks would be insignificant if rendered with the correct motion blur profile.

4.1.1 *Methods.* Thirty-two adult participants completed this experiment. Each participant watched 320 clips. After each animation, participants were asked to rate the naturalness of the animation on a 7-point rating scale (1 = very unnatural, 7 = very natural). A very natural clip was defined as something you would expect to see in the real world. We elected to use a rating scale rather than a forced-choice preference paradigm in order to assess as many clips as possible in the allotted time. Each session lasted approximately 40 minutes.

Experiment 1 also explored the effect of rendering accurate motion-blur profiles and closing amplitudes on the perceived naturalness of eye blinks. In many blink animations, the eyes are fully closed in order to produce a maximum blink amplitude. However, the video data shows large variability in the amplitude of the blinks, with as many as 50% of the observed eye blinks not reaching the fully closed position (quantified as an inter-eyelid distance of zero). Twenty eye blinks were randomly selected from the set of real blinks. Similarly, twenty eye blinks were selected for duration and closing amplitude from a set of 100 eye blinks randomly generated with the PCA model. As a result of the linear model, a small number of generated profiles had negative values and were eliminated from the selection pool. For the fully closed condition (FC), the inter-eyelid distance was normalized to the maximum of the signal, while for the naturally closed (NC) condition, the inter-eyelid distance was normalized by the difference between the maximum and the minimum inter-eyelid distance. Both conditions were animated and then rendered at 300 fps.

To generate the motion blur (MB) effect, the final target frames were obtained by averaging over a window of ten frames centered on the current frame. For the no motion blur condition (NB), the 300 fps blink signal was down sampled to 30 fps by selecting every tenth frame.

In order to investigate the possibility that the complexity of the motion profile should correlate to that of the character as previously proposed [Lasseter 1987], we animated two characters. A professional artist created two 3D computer-generated character heads in Maya (Autodesk). The first was a photorealistic character that was made using photographs and videos of Actor 1 for reference and texture information. The second character was created in a simple cartoon style. For the eye blinks based on tracked data, the Maya blend-shape weighting parameters were based directly on tracked data that was scaled to match the [0 1] interval. The stimuli for the two characters were presented in alternating blocks (photorealistic stimuli block and cartoon stimuli block) with the order for the two blocks randomized.

4.1.2 *Results.* We performed a 2 (character) × 2 (profile) × 2 (motion blur) × 2 (closing amplitude) repeated-measures ANOVA with Bonferroni corrections for multiple comparisons and a significance threshold of $p = 0.05$. There were higher naturalness ratings for the photorealistic character than for the cartoon character, $F(1, 31) = 5.91$, $p = 0.02$ (see Table I). There was a significant main effect of

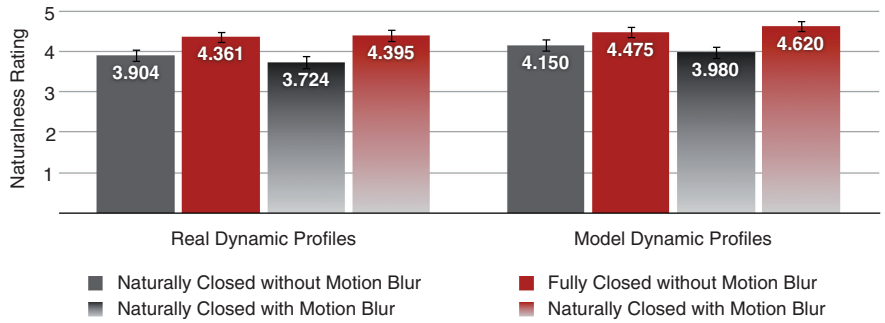


Fig. 9. Experiment 1 results. Naturalness ratings for real and model dynamic profiles with or without motion blur.

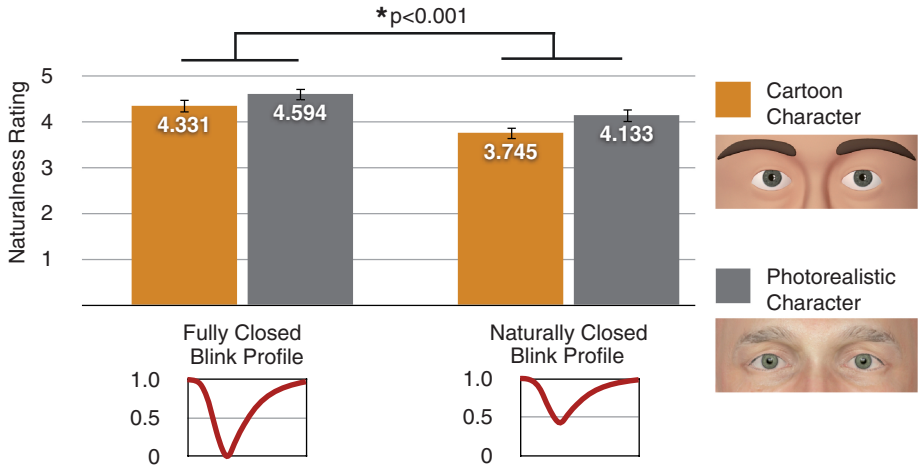


Fig. 10. Experiment 1 results. The effect of closing amplitude on naturalness ratings for the cartoon and photorealistic characters.

profile such that the model blinks were rated as more natural than the real blinks, $F(1, 31) = 39.07$, $p < 0.001$ (Figure 9). There was no main effect of motion blur, $F(1, 31) = 0.95$, $p = 0.34$. A significant main effect for amplitude was found, such that the fully closed blinks received higher naturalness ratings than the naturally closed blinks, $F(1, 31) = 15.55$, $p < 0.001$ (Figure 10). All potential interactions were examined, and two were found significant. There was a significant interaction between blur and amplitude, $F(1, 31) = 20.35$, $p < 0.001$, such that the fully closed blinks received higher ratings with motion blur than without motion blur, but the reverse was true for the naturally closed blinks. There was also a significant interaction among character, blur, and amplitude, $F(1, 31) = 9.93$, $p = 0.004$, suggesting that the ratings for the naturally closed blinks on the cartoon character without motion blur received lower ratings than with motion blur while on the photorealistic character, naturally closed blinks without motion blur were rated higher than with motion blur. However, motion blur increased the ratings for both cartoon and photorealistic characters in the fully closed condition.

### 4.2 Experiment 2: Comparing Model Eye Blinks to Traditional Blink Animation Methods

In this experiment, we contrast naturalness ratings for the animated eye blinks generated from our model with those created using traditional animation techniques, including ease-in/ease-out,

asymmetric linear, and symmetric linear methods. Additionally, we examined the effect of blink duration.

4.2.1 *Methods.* Forty-three adult participants completed this experiment. For each of 400 trials, the participants watched a clip and rated the naturalness of the animation on a 7-point rating scale (1 = very unnatural, 7 = very natural). Each session lasted approximately half an hour.

Clips were created in a 5 (dynamic profile) × 4 (duration) × 2 (character) design. Five categories of blink profiles were included for comparison with our model: symmetric linear (SL), asymmetric linear (AL), an asymmetric ease-in/ease-out (AL Ease), and a symmetric ease-in/ease-out (SL Ease) as described in Section 4. For each category of blinks, five exemplars each were generated for four durations: 7, 9, 11, and 13 frames (for videos shown at 30 fps). In all cases, the eyes fully closed and the motion blur parameters described in Experiment 1 were used. This process resulted in 100 unique blink animations that were then rendered with the photorealistic and cartoon characters. The animations for each character were kept in separate blocks. Each block of 100 clips was shown twice during the experiment, for a total of 400 trials over the course of four blocks.

4.2.2 *Results.* A 5 (profile) × 4 (duration) × 2 (character) repeated-measures ANOVA was performed with Bonferroni corrections for multiple comparisons and a significance level of $p = 0.05$ (see Table II and Figure 11). We found a significant main effect of profile, $F(4, 39) = 11.52$, $p < 0.001$, such that the highest ratings were given to blinks generated with our profile, followed by the AL Ease condition, the SL Ease condition, the AL condition, and finally the SL condition. All pairwise comparisons between different dynamic profiles were significant at $p < 0.05$ (Bonferroni corrected). Additionally, there was a significant main effect for blink duration, $F(3, 40) = 23.40$, $p < 0.001$, such that naturalness ratings were highest for 9 followed by 7, 11, and 13 frames. Pairwise comparisons showed no significant difference between blinks of duration 7 and 9 frames. However, all other pairwise comparisons were significant with $p < 0.05$. The main effect of character was not significant, $F(1, 42) = 0.50$, $p = 0.48$. The interaction among character, profile, and duration was not significant, $F(12, 31) = 0.51$, $p = 0.89$. Overall, the highest average naturalness rating was given for the photorealistic character with the model eye blink profiles and a 9-frame blink duration (mean 4.95). Interestingly, 9 frames was the dominant blink duration in the distribution of blink durations from our tracked data, as shown in Figure 6.

All pairwise interactions were significant, including between character and profile, $F(4, 39) = 3.95$, $p = 0.009$; character and duration, $F(3, 40) = 5.65$, $p = 0.003$; and profile and duration, $F(12, 31) = 4.21$, $p < 0.001$. Although there was a significant character by profile interaction, the naturalness ratings followed the same rank order for both characters such that the ratings for the model blinks were the highest, followed by asymmetric ease-in/ease-out, symmetric ease-in/ease-out, asymmetric linear, and symmetric linear. For the cartoon character, the preferred duration was 7 frames after collapsing across dynamic profiles (mean 4.50) while for the photorealistic character the highest rating is at a 9 frame duration (mean 4.56). This result suggests that appearance plays an important role in determining what is perceived to be natural motion. In fact, according to the type of animation, in some cases it may be desirable for cartoon-like characters to preserve the less natural dynamics in order to emphasize their nonhuman characteristics. The interaction between profile and duration is potentially due to an effect of profile on perceived blink duration. Participants gave low ratings ratings to the 13-frame symmetric linear blinks. Some participants mentioned in informal conversation that those blinks seemed longest. Future work could examine whether perceived duration is affected by profile and, in turn, whether these combined factors affect naturalness ratings.

Table II. Experiment 2 Results

| | Condition | Mean(SE) | F | p |
|---|---|---|---|---|
| Profile | Our Model | 4.57 (0.12) | 11.52 | <0.001 |
| | AL Ease | 4.28 (0.11) | | |
| | SL Ease | 4.04 (0.12) | | |
| | AL | 3.92 (0.12) | | |
| | SL | 3.73 (0.13) | | |
| Duration | 7 frames | 4.46 (0.14) | 23.40 | <0.001 |
| | 9 frames | 4.47 (0.11) | | |
| | 11 frames | 3.94 (0.12) | | |
| | 13 frames | 3.57 (0.13) | | |
| Character | Cartoon | 4.07 (0.11) | .49 | 0.48 |
| | Photorealistic | 4.16 (0.14) | | |

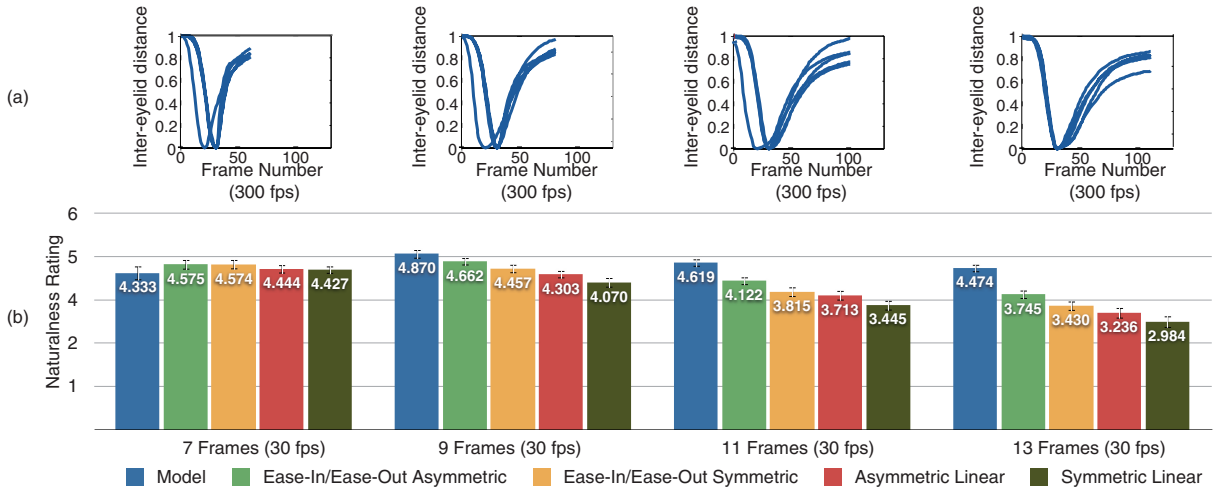


Fig. 11. Experiment 2 conditions and results. (a) Model dynamic profiles for the four different durations used in experiment 2. (b) Average naturalness ratings for the five dynamic profile conditions according to duration.

## 4.3 Experiment 3: Lower Eyelid Motion Contribution

The third study examined the contribution of lower eyelid movements, including horizontal and vertical motion, to perceptions of naturalness.

4.3.1 *Methods.* Twenty adult participants completed this experiment. Participants rated the naturalness of 160 clips on a 7-point rating scale (1 = very unnatural, 7 = very natural). Sessions lasted 20 minutes.

Twenty exemplars for each of four types of clips were created. In the first type, the lower eyelid moved accurately horizontally and vertically (Both). The other conditions included vertical motion only (Vertical), horizontal motion only (Horizontal), and no lower lid motion (None). The horizontal and vertical motion parameters were those originally calculated from our model. All clips had motion blur, and the blink durations followed the natural distribution (Figure 6). All clips were rendered on the photorealistic character because the cartoon was not capable of horizontal lower lid motion. Participants saw two randomly ordered blocks, each containing all of the possible combinations of lower eyelid motion, resulting in two viewings of each clip.

Table III. Experiment 3 Results

| Lower Lid Dynamics | Mean(SE) | F | p |
|---|---|---|---|
| Both | 4.45 (0.83) | 1.28 | 0.31 |
| Vertical | 4.41 (0.92) | | |
| Horizontal | 4.51 (0.86) | | |
| None | 4.46 (0.89) | | |

4.3.2 *Results.* We performed a 4 (lower eyelid motion type) $\times$ 1 repeated-measures ANOVA with Bonferroni corrections for multiple comparisons and a significance level of 0.05 (see Table III). There was no significant effect of the various types of lower eyelid motion on perceived naturalness, $F(3, 17) = 1.28$, $p = 0.31$. The result suggests that viewers are not sensitive to this motion on our characters at the presented scale.

## 5. DISCUSSION

Our perceptual studies underline the importance of using profiles of blinks that are based on a physiologically valid model rather than those created using simple animation curves. In experiment 1, viewers rated the blinks animated using our model as more natural than those animated using measured blink profiles. We hypothesize that this is because the PCA model blinks were closer to the prototypical mean blink from the training set. Participants found fully closed blinks to be more natural than naturally closed blinks. This result may have arisen because viewers were unaware that the eyelids often fail to close fully during blinks and/or because this phenomenon is more obvious in animated characters. We also suspect that the effect may be a result of observing blinks independently rather than in a sequence. In future studies, we intend to investigate the naturalness of blink sequences. As expected, the participants found the blinks of the photorealistic character to be more natural than those of the cartoon character.

In our experiments, the blink models were derived from one actor's data (Figure 6: Actor 1). Our intention was to closely match the photorealistic character to the actor's features. Because the dynamic eye blink profiles across three different actors shown in Figure 6 appear to be similar, we postulate that the results generalize. As an extra validation in future studies, we intend to compare eye blinks derived from different actors. In particular, we are interested in age correlates and the percentage of fully closed eye blinks in an actor's dataset. Another avenue that we plan to explore in future experiments is left/right eye blink symmetry and the correlation with naturalness ratings. Our system is capable of tracking both eyes simultaneously. In most situations, the left and right eyelid dynamics are highly correlated and we created our models and animations using data from only one eye in this study. However, we noticed occasional asymmetries in our video recordings that we would like to examine further.

The second experiment compared blinks generated from our model to those generated from simple profiles, including asymmetric linear profiles, symmetric linear profiles, asymmetric profiles with ease-in/ease-out curves, and symmetric profiles with ease-in/ease-out curves (Figure 8). The model blinks were rated as significantly more natural than the simple approximations. Viewers also compared these blinks at various durations. The highest naturalness ratings were assigned to blinks generated from our model that were nine frames in duration. Experiment 3 results suggest that there is no effect of the various possible techniques for lower eyelid motion on our 3D characters; this knowledge is particularly beneficial for animators using simple models that do not have the capability for this type of movement.

From a methodological perspective, this article introduces a new technique for detecting and describing blinks in video recordings. High-resolution spatial and temporal information were collected with a high-speed video camera. Then, AAMs were used to track the eyes and measure the blink profiles

in long videos. The inter-eyelid distance during blinks was used to construct a PCA-based model that can generate eye blink dynamic profiles with properties (duration, closing amplitude) similar to the original distribution. Once the PCA-based blink model has been created, it can generate a variety of physiologically valid blink profiles for use in animation.

Our model is easy to include in an animation pipeline. For example, a script can be used to generate a variety of blinks for a character. Animation curves can then be driven from these dynamics. Technical directors can create a blink button and seamlessly use this system without increasing the time required for animation. Additionally, the model can create variations in the blink sequences, an important component in making animations as true-to-life as possible. A limitation of our studies is that participants gave naturalness ratings of individual eye blinks in isolation: no facial context was given, and no inter-blink timing was considered. In the future, we intend to generate full facial animations that show sequences of eye blinks. Future work will require improving our facial animation system to allow for small, subtle changes in the face (such as breathing) to match observations of faces in video. Additionally, we also intend to utilize the framework presented earlier to investigate blink frequency patterns and their correlations to head motion and facial expressions.

## ACKNOWLEDGMENTS

The authors would like to thank the APGV reviewers, Lavanya Sharan, Jeffrey Cohn, Betty Mohler, and James McCann for their feedback and Moshe Mahler for the Maya modeling work.

## REFERENCES

BACHER, L. AND SMOTHERMAN, W. 2004. Spontaneous eye blinking in human infants: A review. *Devel. Psychobiol. 44*, 95–102.

BACIVAROV, I., IONITA, M., AND CORCORAN, P. 2008. Statistical models of appearance for eye tracking and eye-blink detection and measurement. *IEEE Trans. Consum. Electron.* 1312–1320.

BAKER, S., GROSS, R., AND MATTHEWS, I. 2003. Lucas-Kanade 20 years on: A unifying framework: Part 3. Tech. rep. CMU-RI-TR-03-35, Robotics Institute, Carnegie Mellon University, Pittsburgh, PA.

BLOUNT, W. 1928. Studies of the movements of the eyelids of animals: Blinking. *Quart. J. Exper. Physiol. 18*, 111–125.

CAFFIER, P. P., ERDMANN, U., AND ULLSPERGER, P. 2003. Experimental evaluation of eye-blink parameters as a drowsiness measure. *Euro. J. Appl. Phys. 89,* 3–4, 319–325.

CODISPOT, M., BRADLEY, M. M., AND LANG, P. J. 2001. Affective reactions to briefly presented pictures. *Psychophysiol.* 38, 474 – 478.

COOTES, T. F., EDWARDS, G. J., AND TAYLOR, C. J. 1998. Active appearance models. In *Proceedings of the European Conference on Computer Vision*. 484–498.

CULHANE, S. 1988. *Animation from Script to Screen*. St. Martin's Press.

DARGIS, M. 2007. Confronting the fabled monster, not to mention his naked mom. *New York Times* (11/16/07).

DENG, Z., LEWIS, J. P., AND NEUMANN, U. 2005. Automated eye motion using texture synthesis. *IEEE Comput. Graph. Appl. 25,* 2, 24–30.

DOUGHTY, M. J. 2001. Consideration of three types of spontaneous eyeblink activity in normal humans: During reading and video display terminal use, in primary gaze, and while in conversation. *Optom. Vis. Sci. 78,* 10.

EVINGER, C., MANNING, K. A., AND SIBONY, P. A. 1991. Eyelid movements: Mechanisms and normal data. *Investig. Opthal. Vis. Sci. 32,* 2, 387–400.

EVINGER, C., SHAW, M. D., PECK, C. K., MANNING, K. A., AND BAKER, R. 1984. Blinking and associated eye movements in humans, guinea pigs, and rabbits. *J. Neurophysiol. 52,* 2, 323–339.

GUITTON, D., SIMARD, R., AND CODERE, F. 1991. Upper eyelid movements measured with a search coil during blinks and vertical saccades. *Investig. Ophthal. Vis. Sci. 32,* 13, 3298–3305.

LASSETER, J. 1987. Principles of traditional animation applied to 3d computer animation. *Comput. Graph.* 35–44.

LEAL, S. AND VRIJ, A. 2008. Blinking during and after lying. *J. Nonverbal Behav. 32,* 4, 187–194.

LEE, S. P., BADLER, J. B., AND BADLER, N. I. 2002. Eyes alive. *ACM Trans. Graph. 21*, 637–644.

MAESTRI, G. 1996. *Digital Character Animation*. New Riders Publishing.

MATTHEWS, I. AND BAKER, S. 2004. Active appearance models revisited. *Int. J. Comput. Vis. 60,* 2, 135–164.

PORTER, S. AND TEN BRINKE, L. 2008. Reading between the lies identifying concealed and falsified emotions in universal facial expressions. *Psychol. Sci. 19*, 5, 508–14.

STEPTOE, W., OYEKOYA, O., AND STEED, A. 2010. Eyelid kinematics for virtual characters. *Comput. Anim.Virtual Worlds 21*, 161–171.

SUN, W. S., BAKER, R. S., CHUKE, J. C., ROUHOLIMAN, B. R., HASAN, S. A., GAZA, W., STAVA, M. W., AND PORTER, J. D. 1997. Age-Related changes in human blinks. *Investig. Opthal. Vis. Sci. 38,* 1, 92–99.

TANAKA, Y. AND YAMAOKA, K. 1993. Blink activity and task difficulty. *Perceptual Motor Skills 77*, 1, 55–66.

VANDERWERF, F., BRASSINGA, P., REITS, D., ARAMIDEH, M., AND ONGERBOER DE VISSER, B. 2003. Eyelid movements: Behavioral studies of blinking in humans under different stimulus conditions. *J. Neurophysiol. 89,* 5, 2784–2796.

VELTMAN, J. A. AND GAILLARD, A. W. K. 1998. Physiological workload reactions to increasing levels of task difficulty. *Ergonom. 41*, 656–669.

WILLIAMS, R. 2001. *The Animator's Survival Kit*. Faber and Faber.

WILSON, G. F., PURVIS, B., SKELLY, J., FULLENKAMP, P., AND DAVIS, I. 1987. Physiological data used to measure pilot workload in actual flight and simulator conditions. *Hum. Factors Ergonom. Soc. Ann. Meet. Proc. 31,* 7, 779–783(5).

Received April 2011; accepted July 2011